Hindawi
International Transactions on Electrical Energy Systems
Volume 2022, Article ID 5233620, 18 pages
https://doi.org/10.1155/2022/5233620

Research Article

Optimal Coordination of TCSC and PSS2B Controllers in Electric Power Systems Using MOPSO Multiobjective Algorithm

Mehrdad Ahmadi Kamarposhti,[1] **Hassan Shokouhandeh**,[2] **Yahya Gholami Omali**,[3] **Ilhami Colak**,[4] **Phatiphat Thounthong**,[5] **and William Holderbaum**[6]

[1]*Department of Electrical Engineering, Jouybar Branch, Islamic Azad University, Jouybar, Iran*
[2]*Department of Electrical Engineering, Semnan University, Semnan, Iran*
[3]*Department of Electrical Engineering, Hadaf Institute of Higher Education, Sari, Iran*
[4]*Department of Electrical and Electronics Engineering, Faculty of Engineering and Architectures, Nisantasi University, Istanbul, Turkey*
[5]*Renewable Energy Research Centre (RERC), Department of Teacher Training in Electrical Engineering, Faculty of Technical Education, King Mongkut's University of Technology North Bangkok, Pracharat 1 Road, 1518, Bangsue, Bangkok 10800, Thailand*
[6]*School of Science Engineering and Environment, University of Salford, Salford, UK*

Correspondence should be addressed to Mehrdad Ahmadi Kamarposhti; mehrdad.ahmadi.k@gmail.com

Received 10 March 2022; Revised 6 November 2022; Accepted 15 November 2022; Published 28 November 2022

Academic Editor: Sujin Bureerat

Oscillations are an intrinsic phenomenon in interconnected power systems, leading to steady-state stability, safety decline, transmission power limitation, and electric power systems' ineffective exploitation by developing power systems, particularly by connecting these systems to low-load lines. In addition, they affect the economic performance of the systems. In this study, PSS2B power system stabilizers and TCSC compensators are used to improve the stability margin of power systems. In order to coordinate TCSC compensators, the MOPSO multiobjective algorithm with integral of the time-weighted absolute error (ITAE) and figure of demerit (FD) objective functions was used. The MOPSO algorithm optimization results are compared with nondominated sorting genetic algorithm (NSGAII) and multiobjective differential evolution (MODE) algorithms. The optimization results indicated a better performance of the proposed MOPSO algorithm than NSGAII and MODE. The simulations were iterated in two scenarios by creating different loading conditions in generators. The results indicated that the proposed control system, where the coordination between PSS2B power system stabilizers and TCSC compensators using the MOPSO algorithm, is better than power systems in which PSS2B Stabilizers or TCSC compensators are utilized solely. All criteria, e.g., ITAE, FD, maximum deviation range, and the required time for power oscillation damping in hybrid control systems, have been obtained. This means more stability and accurate and proper performance.

1. Introduction

The expansion of power systems, particularly connecting these systems to low-load lines, leads to steady-state stability limitation, safety decline, transmission power limitation, and power systems' ineffective exploitation, affecting the system's economic performance. For damping these oscillations and improving the dynamic stability and the steady-state power system, proper control should be exercised in the system, which could be carried out through the machine excitation control or the reactive power compensators control [1]. The synchronous machine excitation control is possible using different methods. One of these methods uses an auxiliary control loop on the machine excitation known as power system stabilizers (PSSs). One of the chief problems in the stabilizer of conventional power systems is that such a stabilizer is designed merely for particular operating conditions and cannot respond properly under a wide range of

operating conditions. A new generation of power systems stabilizer, called power system stabilizer Two Band PSS2B, with two inputs of reactive power changes and rotational velocity changes, will be used in this study. Compared to the PSS stabilizer, the mentioned stabilizer can demonstrate a more proper performance in a wide range of operating conditions, damping low-frequency oscillations [2]. Besides, we can use FACTS equipment to improve power systems' stability and eliminate the existing constraints in electric power transmission. FACTS equipment is capable of controlling the components of active and reactive transmission powers in transmission lines. Thereby, on-time controlling of these components can lead to a dynamic stability improvement in a power network. Thyristor controlled series capacitor (TCSC) controls the power passing through the line and allows more power passage by controlling the line impedance [3]. In [4], the parameters of the PSSs are selected by the genetic algorithm. In this regard, first, the contribution coefficients are used to determine the stabilizers' placement. Then, the number of stabilizers is reduced using the genetic algorithm, providing an optimal stabilizer model. Although several studies have been conducted on the design, placement, and coordination of power systems stabilizers (PSSs), such stabilizers have merely one proper operating condition. By a change in the conditions of generators, it will encounter a disruption. The next generations of PSS are multiband PSSs, e.g., PSS2B, PSS3B, and PSS4B. Most power system stability studies are related to PSS, and there have been low investigations in the realm of PSS2B. In [5], PSS2B has been used in the power system. This stabilizer shows better performance than the PSS stabilizer.

Some other researchers made efforts in various FACTS equipments in power systems. Being various, the FACTs equipment has been the subject of concern in numerous studies. According to [6], the optimal placement of TCSC in standard power systems with 30 buses is performed using the PSO algorithm. The optimal placement aims to achieve the maximum total transfer capability (TTC), minimizing the power loss in uncontrollable or illegal electric power markets via bilateral and multilateral transactions. A bilateral transaction takes place between a seller and a buyer without the involvement of a third party. The proposed method of [6] happens during two scenarios: one considers bilateral transactions, and the other takes account of the multilateral transaction. In each scenario, three objective functions will be investigated. The first objective function consists of TTC maximization and minimizing losses, the second one includes TTC maximization, and the third one consists of loss minimization. The results indicate that in the presence of TCSC, the total transmission power capacity increases, whereas the active power loss declines. According to [7], for TCSC placement, the improved particle swarm algorithm has been used in the power system. In this reference, TCSC is considered distributed. In this article, the proposed method experiments on two networks with 14 and 118 bus bars. In order to validate the proposed method, the simulation is performed using eight other algorithms. The results indicate that the proposed method in this study has better results compared to other algorithms.

In [8], a local fuzzy-based damping controller (LFDC) is used to improve the transient stability of the power system. In this study, in order to perform the proposed design, the accurate TCSC model is used based on its actual behavior. LFDC uses the frequency as a feedback signal for the phase-fired control (phase angle control). Fuzzy controller parameters are adjusted using a chaotic optimization algorithm. The proposed method's results were compared with other methods, indicating that the proposed LFDC is an efficient tool for transient stability improvement; that is, because it merely uses local signals, easily accessible. According to [9], the placement and adjustment of SVC and TCSC parameters were performed, aiming to improve the small-signal stability of the power system. The particle swarm algorithm is used to solve the problem. In order to validate the proposed algorithm, the simulation was performed in a system by considering two states: two probabilistic events such as load enhancement and line disconnection. The results indicate that compared to SVC, the TCSC controller is more effective even at the time of more loading to overcome small-signal stability problems. According to [10], the neural network-based adaptive neuro-fuzzy inference system (ANFIS) method is used for TCSC design to increase the power system stability. This research aims to improve the rotor angle stability and the system's voltage profile. In order to improve the total performance of the system, there are various methods to optimally coordinate this equipment. A number of provided methods are nonlinear and complex [11], while other methods are linearized based on the model of a system [12]. According to [13], the nonlinear optimization method has been used to minimize the mutual effects of TCSC and PSS. Compared to linear methods, nonlinear methods require more time to obtain a response. According to [14], PSS and SCCC combination is used in the power system to create the required damping for low-frequency oscillations (LFOs). In this study, the combined bacterial foraging and particle swarm algorithm is used to optimally search for the control parameters of the PSS and SCCC combined system. The proposed method is provided on the sample system by applying different loading conditions and system adjustments to demonstrate its effectiveness. The results demonstrate that the proposed controllers lead to a decline in the power system oscillations under a wide range of operational conditions and different disruptions. In addition, the simulation results indicate that in a multimachine power system, modal oscillations are effectively neutralized by the proposed method. Also, according to [9], the SVC compensator and the optimized TCSC by PSO algorithm are used, aiming to mitigate small-signal oscillations in a multipurpose power system. Making use of PSS in generators is for reducing the regular power oscillations. However, the performance of this system is subject to changes in network adjustment and load change. Besides, installing FACTs equipment is a proper proposal to reduce oscillations. Also, in this study, two states are considered for the system: transmission line disconnection and load enhancement. The results demonstrate that using the proposed method brings about proper stability in small signal. According to [15], PSS and TCSC are used,

whereas PSO algorithms are used for coordination. In this method, a wide range of operating conditions is considered for the system. The results indicate that the proposed coordinated controllers have a great level of capability in oscillations reduction among the power systems range, significantly raising the dynamic stability of those systems. Additionally, the proposed model is superior to both the uncoordinated designed PSS stabilizer and TCSC controller.

The simultaneous usage of TCSC and PSS in [16] improves the stability of the power system under investigation. In order to optimally controlling TCSC and PSS, the ant colony algorithm (a stochastic selection-based system) is used. Single machine infinite bus system (SMIB) is exposed to different operating conditions and disruptions so that the effectiveness of the proposed control method is demonstrated. The simulation results indicate that the proposed method is effective in a system's stability, superior to similar methods. According to [17], an active power-based sensitivity method is used to the optimal place of TCSC. Also, for better TSCS performance, proper input signals are determined. In addition, the proper design of the power oscillation damper (POD) and PSS and POD systems coordination were separately investigated on different scales. In this study, the coordination problem of POD-TCSC and that of POD-TCSC and PSS has become a multiobjective optimization problem, solved using a particle swarm optimization algorithm. The proposed method was applied on a 16-machine 68-bus network. The simulation results indicate a strong and satisfactory performance in the local and interregional oscillations of power systems. Bacteria foraging algorithm is among other algorithms used in the last papers due to its higher accuracy in finding more optimal points. According to [18], the coordination was performed between PSSs and a static VAR compensator (SVC) by bacteria foraging algorithm. Ultimately, by coordinating between controllers in the power system, the interregional oscillations obtain acceptable damping. This algorithm was also used in [19] to optimally design the power system stabilizer. The improved version of this algorithm was used in [20] for optimally designing PSS stabilizers and TCSC. This study asserts that the improved version of the BFOA algorithm has higher convergence accuracy and velocity. The cultural algorithm is among the other algorithms used to design PSS. The duck pack algorithm was used in [21] to determine the PSS parameters in the lead-lag power systems. In this article, an objective function is defined based on eigenvalues placement by which the algorithm aims to provide the power systems' stability in a wide range of generator's operating conditions. The obtained results by the duck pack algorithm have been compared with the results of the particle swarm algorithm. The duck pack algorithm is also used in [22] to design the stabilizers in 3-Machine power systems, whose results are compared with the optimized genetic algorithm. The results indicate that the duck pack algorithm has a better performance compared to the genetic algorithm. In [23], the effect of optimal design of the PSS and their coordination has been studied practically. The results showed that in case of improper selection of the PSS coefficients, there is a possibility of power system instability. Additionally, in [24] the presence of a TCSC compensator in the power system was evaluated experimentally. Studies have shown that the presence of TCSC improves the parameters of the transmission line and if the optimal selection of its control coefficients, the dynamic stability of the power system is increased.

The search optimum algorithm (SOA) was used in [25], aiming to optimally design PSSs and coordinate them with a static synchronous series compensator (SSSC). A new objective function is used in this article. The proposed objective function is a function of weighting factors from two ITAE objective functions and a function combined with overshoot, undershoot, and settling time. This study asserts that the designed stabilizer performs more accurately by minimizing the proposed objective function compared to the other methods. The PSS coordination in [26] is to reduce the interregional mode oscillations by a combined method of optimization and eigenvalues sensitivity analysis. This combination allows for designing a different PSS, where the objective function is minimized as much as possible. In order to prove the strength of the proposed method, the designed stabilizer is used in a system with 69 generators. In [27], the hybrid particle swarm optimization (HPSO) algorithm and gravitational search algorithm (GSA) are employed to design PSS and coordinate PSS and static synchronous series compensator (SSSC). Compared to the GSA and PSO algorithms, hybrid algorithms are of higher accuracy. The results of the simulation carried out on multimachine systems indicate the robust performance of the designed control system in damping low-frequency oscillations. In [28], stabilization through multiple signals is investigated such that each installed stabilizer operates through the signals that communication lines from another region have sent. Depending on telecommunication platforms, receiving noise and delay are disadvantages of this method. In reference [29], stabilization of the power system is carried out using the controllers based on fuzzy logic. The controller proposed by this paper is a hybrid fuzzy and PID stabilizer that stabilized the power system under uncertainty. Optimal selection of PID controller coefficients will increase the accuracy of the controller [30]. Reference [31] has had an overall review of various methods of oscillation control in power systems and stability improvement of power systems. Besides, in this article, various PSSs and their design methods are categorized.

In this paper, the optimal coordination of PSS2B and TCSC is carried out to improve the power system dynamic stability. In addition, the integral of the time-weighted absolute error (ITAE) and figure of demerit (FD) indices were selected as objective functions, and the modified version of particle swarm optimization (MOPSO) algorithm is proposed to solve the optimization problem.

In the following, the power system model is explained in Section 2, and the PSS2B stabilizer is introduced in Section 3. The problem modeling, objective function, and problem constraints are presented in Section 4. In Section 5, the multiobjective particle swarm algorithm is briefly explained. The simulation results are presented in the form of two scenarios in Section 6. Finally, presenting results, this article ends in Section 7.

2. Power System Model

Several models are proposed to illustrate the dynamic performance of a power system. The Heffron and Phillips model is one of the most mainly used dynamic models of the power system. The Park's equations for the 4th order model of a power system can be formulated as following equations [32]:

$$\begin{aligned} U_d &= U_T \sin\ \delta_m = \frac{U_B}{A}\sin(\delta_m + \alpha) + \frac{B}{A} i_d \cos(\beta - \alpha) - \frac{B}{A} i_q \sin(\beta - \alpha) = \ X_q i_q - R_A i_d, \\ U_q &= U_T \cos\ \delta_m = \frac{U_B}{A}\cos(\delta_m + \alpha) + \frac{B}{A} i_d \sin(\beta - \alpha) + \frac{B}{A} i_q \cos(\beta - \alpha) = E'_q - \ X'_d i_d - R_A i_d, \end{aligned} \tag{1}$$

where R_A, X'_d, and X_q are armature resistance, d-axis transient, and q-axis reactance, respectively. Also, i_d is d axes stator current, and i_q is q axes stator current. The linearized model of the power system can be formulated as following equations:

$$\begin{aligned} \Delta\dot{\delta} &= \omega_0 \Delta\omega, \\ \Delta\dot{\omega} &= \frac{1}{2H}\left(\Delta P_M - K_D \Delta\omega - K_1 \Delta\delta - K_2 \Delta\acute{E}_q\right), \\ \Delta\dot{E}_q &= \frac{1}{\acute{T}_{do}}\left(\Delta E_{f\,d} - K_3 \Delta\acute{E}_q - K_4 \Delta\delta\right), \\ \Delta\dot{E}_{f\,d} &= \frac{1}{T_e}\left[K_e\left(\Delta V_R - K_5 \Delta\delta - K_6 \Delta\acute{E}_q\right) - \Delta E_{f\,d}\right], \end{aligned} \tag{2}$$

where H is inertia constant, K_D is the damping torque parameter, T_{do} is d-axis transient open circuit time constant, and T_A and K_A are automatic voltage regulator (AVR) gain and time constant, respectively. Therefore, the Heffron-Phillips model of a single machine with a power system stabilizer can be shown in Figure 1.

In Figure 1, K_1 to K_6 are Heffron-Phillips model constants and their values are dependent on the power system parameters and its operating conditions. The constant K_3 is only a function of the parameters. The K_5 is dependent on external series impedance and its value plays an important role in the effect of the AVR on damping torque. The Heffron-Phillips model for a multimachine power system is an extended version of a single-machine power system. In Figure 2, the phasor diagram of i^{th} machine for a multimachine power system is shown.

In Figure 2, X-Y axis and $d_i - q_i$ axis stands for the system and i^{th} generator coordinates, respectively. Also, δ_i is the difference of phase angle between d_i and X which changes permanently. The Heffron-Phillips model of i^{th} machine is shown in Figure 3.

3. PSS2B Stabilizer

PSS is a device that improves the dynamic performance of a power system by adding auxiliary signals to the excitation system. This stabilizer usually feeds on the signals, such as angular velocity changes, frequency, generator terminal power, or a combination of these signals. The output of these stabilizers is a voltage signal applied on excitation to favorably affect the dynamic performance of a power system by damping its oscillations. Another model of IEEE standard stabilizers is the PSS2B stabilizer. This stabilizer has two inputs of Δw and P_e. In Figure 4, a block diagram of the PSS2B stabilizer is indicated.

Similar to the lead-lag stabilizer, a sensor, washout, gain, and limiter of the output voltage are employed in the structure of PSS2B. A transformer is employed in the input of this stabilizer. This transformer is indicated in Figure 5.

The input of this stabilizer is angular velocity changes and active power of generator output.

4. Problem Modeling

For this purpose, two criteria of ITAE [33] and FD [34] have been employed as the objective function for designing stabilizers and coordination.

$$\mathrm{ITAE} = 1000 \int_0^{t_{\mathrm{sim}}} t.\left(|w_1 - w_2| + |w_1 - w_3| + |w_1 - w_4| + |w_3 - w_4|\right), \tag{3}$$

$$FD = (\mathrm{OS} \times 5000)^2 + (\mathrm{US} \times 5000)^2 + T_s^2. \tag{4}$$

In (3), w is the angular velocity of the generator, and t is the operator of time. In (4), OS is the maximum value of overshoot, the US is undershot, and T_s is a damping time of oscillations. In this case, it can be stated that ITAE is a suitable criterion for damping of interregional oscillations, and FD is a criterion for separately minimizing oscillations of each generator. In equation (3), $\Delta\omega$ is generators' angular velocity change, and t is the operator of time. Besides, in equation (4), the US, OS, and T_s parameters are maximum overshoot, undershoot, and settling time.

A TCSC module consists of a fixed series capacitor parallel to the thyristor-controlled reactor (TCR), which is indicated in Figure 6. A TCR consists of a series reactor with two-way thyristor switches, which ignites at α phase between 90 to 180 degrees to be in the capacitive phase. Suppose that TCSC is installed on the commutation line between two buses of i and j, in which TCSC is modeled as a continuous capacitive reactance.

Therefore, the passing-through flow will be as follows:

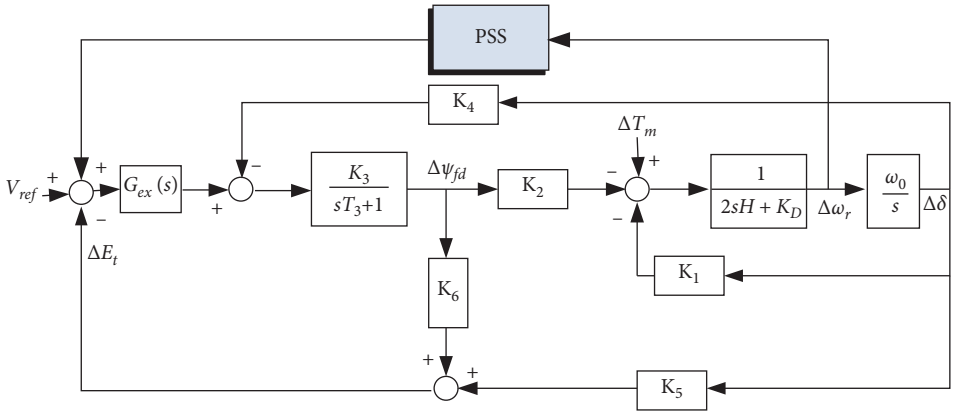

Figure 1: Heffron-Phillips model of the study SMIB system.

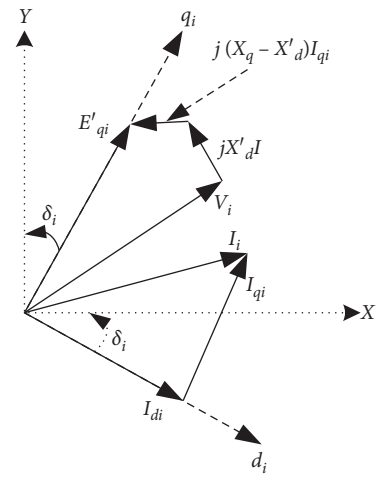

Figure 2: Phasor diagram of a multimachine power system.

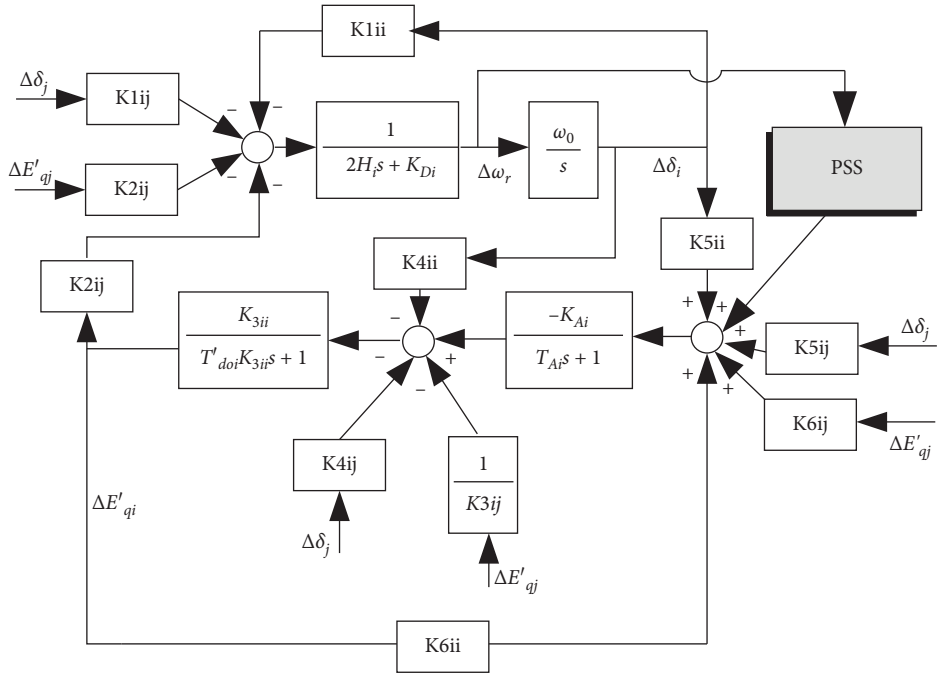

Figure 3: A multimachine power system Heffron-Phillips model.

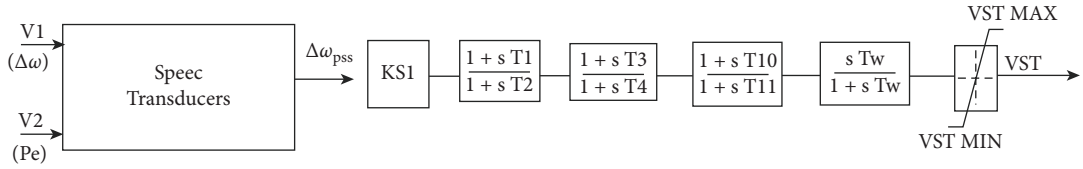

Figure 4: Block diagram of PSS2B stabilizer.

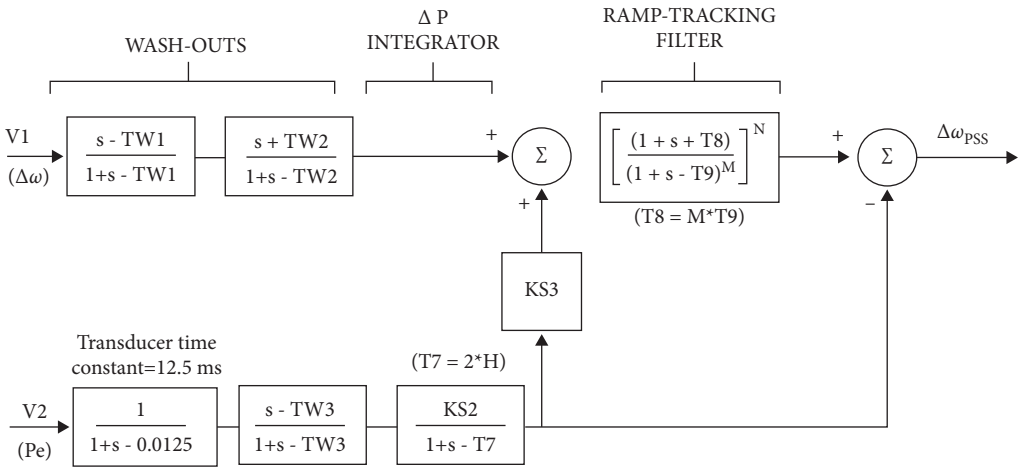

Figure 5: Block diagram of speed transformer of PSS2B stabilizer.

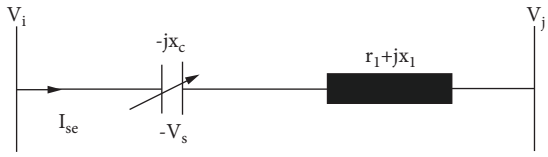

Figure 6: TCSC compensator installed on commutation lines.

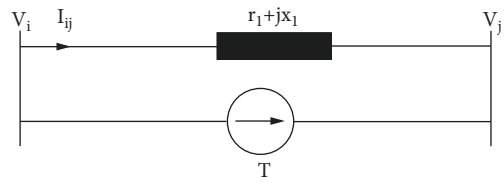

Figure 7: Replacement of voltage source with flow source.

$$I_{se} = \frac{V_i - V_j}{r_l + j(x_l - x_c)}. \tag{5}$$

The injected flow of the TCSC model is calculated by equation (6) by replacing the voltage source with the flow source:

$$I_s = \frac{V_S}{r_l + jx_l} = -\frac{jx_c I_{se}}{r_l + jx_l}. \tag{6}$$

In Figure 7, the replacement of the voltage source with the flow source is modeled, and the TCSC flow source is indicated in Figure 8. Injected flow to i and j groups is calculated as follows:

$$I_{si} = \frac{jx_c}{r_l + jx_l}.\frac{V_i - V_j}{r_l + j(x_l - x_c)} = -I_{sj}. \tag{7}$$

The damping controller is designed in TCSC to generate electric moment in the phase, proportional to the deviation of angular velocity. The lead-lag transfer function is one of the suggested methods to be employed as a controller in TCSC. The structure of TCSC along with its controller is indicated in Figure 9. The performance of the TCSC

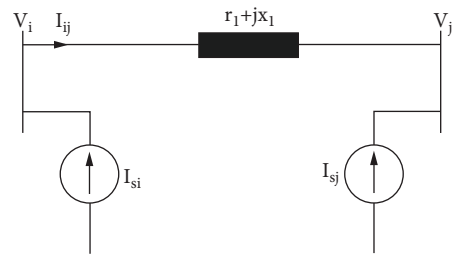

Figure 8: The model of flow injection for TCSC.

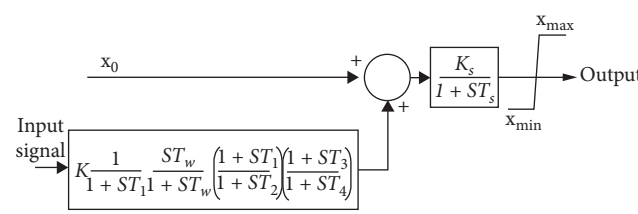

Figure 9: TCSC block diagram along with the controller.

compensator highly depends on its controller parameters. In this thesis, a multiobjective particle swarm algorithm is employed. Many input signals have been proposed for TCSC. However, a signal that consists of valuable information from interregional modes is suitable. In Figure 9, X_0 is a reference impedance that is determined by the designer and is always constant.

The variation range of decision-making variables (parameters of PSS2B stabilizers and TCSC controller) is presented in Table 1.

It is necessary to coordinate the PSS2B and TCSC to prevent negative interactions between them. The coordination can be carried out by optimally adjusting the coefficients of the TCSC controllers and the PSS2B parameters. Therefore, appropriate objective functions and optimization algorithms must be used to create coordination.

5. The Steps of Multiobjective Particle Swarm Algorithm

Particle swarm optimization (PSO) was introduced by Kennedy and Eberhart in 1995. In the PSO algorithm, several particles are scattered in the search space. Each particle calculates the value of the objective function in the position of the space where it is placed. Afterwards, it selects a direction for movement by combining the information of its current position and the best position it has ever been and information of one or several particles among the best particles existing in the population. After performing a group movement, one-step of the algorithms becomes complete. These steps are repeated several times until the desired answer is obtained. Particle i in the space has the following five features:

(1) Position of particle i at iteration t

(2) Objective function corresponding to that position

(3) Velocity of particle i at iteration t

(4) The best position experienced by particle i at iteration t

(5) Objective function corresponding to this best position

Accordingly, the velocity and position of particle i at each repeat are updated by the following equations [34]:

$$V^i[t+1] = wv^i[t] + c_1 r_1\left(x^{i\text{best}}[t] - x^i[t]\right) + c_2 r_2\left(x^{g\text{best}}[t] - x^i[t]\right),$$
$$x^i[t+1]x^i[t] + v^i[t+1], \tag{8}$$

where c_1 and c_2 are personal and group learning, respectively, and have values between zero and two. Additionally, r_1 and r_2 are random in the interval of 0 to 1, and w is the inertial weight, which is between 0.4 and 0.9. Selecting a constant coefficient, w will reduce the accuracy of the algorithm. In the proposed version of the PSO algorithm, the w changes dynamically in each iteration.

$$W = W_{\max} - \frac{W_{\max} - W_{\min}}{iter_{\max}} \times \text{iter}. \tag{9}$$

Table 1: Variation range of parameters.

K	[1, 30]
T_{n1}	[0.1, 1]
T_{d1}	[0.1, 1]
T_{n2}	[0.1, 1]
T_{d2}	[0.1, 1]

Figure 10 indicates the adjustment of velocity and the new position of each particle at the end of each repeat.

The difference between the PSO and MOPSO algorithms is in determining the best particle and best experience. The selection of the best personal experience (P_{best}) and best swarm experience (G_{best}) is carried out according to a specific mechanism. A multiobjective algorithm cannot select P_{best} and G_{best} as the best answer because all dominant answers are at the same level of superiority. P_{best} merely appears when a new particle dominates its previous value. G_{best} is also selected at each repeat among the dominant answers existing in the archive or repository.

In this algorithm, a parameter titled repository or archive of answers is employed that is indicated by rep (repository). This parameter is a population of no dominated answers that are stored outside the algorithm. These answers are separate from the main population and are of limited capacity. According to Figure 10, each particle has three information sources in the search space as follows:

(1) Previous velocity

(2) Tendency to the best personal experience

(3) Tendency to the best swarm experience

As mentioned earlier, the concept of the best swarm experience is different in the MOPSO algorithm. Each particle randomly selects a leader from the rep section every moment. In the classic PSO algorithm, only one member in the space can be selected as a leader due to the single-objective nature of the problem. However, there are several members in this algorithm; thus, one of the rep members is selected instead of the best swarm experience.

Figure 11 demonstrates a search space where 22 members are scattered. In this figure, the members that are highlighted can be selected as a leader because these members will not be dominated by any other member. However, do all leaders have an identical value?. A leader must be selected that helps order and arrangement of answers, or in other words, is located in less occupied places of the space. In order to consider the factor of making order and arrangement, the search space is divided into networks [35].

In order to compare leader members, first, the region-based selection is carried out instead of the individual-based selection. In other words, first, the best region or house is selected, and then a member of that house is selected. In Figure 11, the six houses (houses 13, 14, 15, 21, 22, and 31) are members of the rep. As can be seen, the fourth house is the most populated (mostly populated), and it is less possible to be selected. In general, it can be claimed that the selection possibility of houses with a lesser population is more in this process. In comparison, the selection possibility of houses

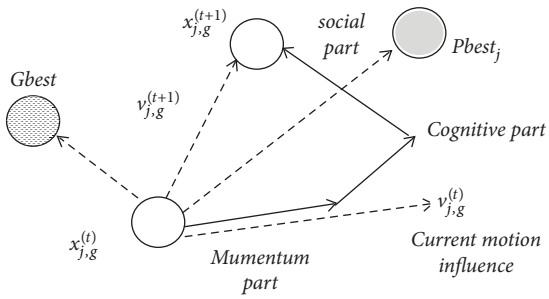

Figure 10: Adjustment of position and velocity of particles in the PSO algorithm.

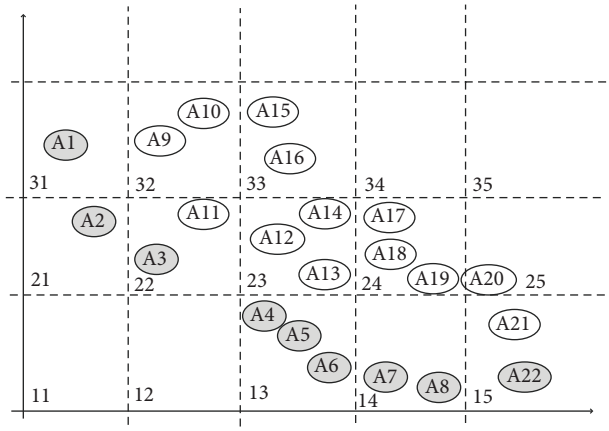

Figure 11: The view of network search space.

with a greater population is more. This selection can be carried out by a discrete distribution, and sampling from this discrete distribution is performed using the roulette wheel method [36].

The steps of multiobjective PSO algorithms are listed as follows:

(1) Creation of initial population

(2) Separating no dominated population and storing them in rep

(3) Tabulation of the discovered target space

(4) Each particle selects a leader from rep members and continues its movement

(5) The best personal experience of each particle is updated

(6) No dominant members of the current population are the added to rep

(7). Dominant members of rep are eliminated

(8) If the number of rep members is more than the determined capacity, the main members are removed

(9) If the ending condition is not met, return to step 3; otherwise, finish

In the MOPSO algorithm, the limited external archive stores nonpost answers. To find optimal answers, particle groups must not scatter in specific spots in order to be able to cover the whole search space. For this purpose, nonpost answers that have greater swarm distance values are accorded a higher priority in this method. In the external archive, nonpost answers are ordered according to swarm distance value and in a descending way. In this case, an answer is randomly selected from several answers from the top of the archive (for instance, the top 10% of the archive) at each step. This descending order in the external archive helps us elsewhere when the archive is full. Under such circumstances, an answer is randomly selected from nonpost answers from the bottom of the archive (for instance, the bottom 10%) and is replaced by a new nonpost answer found in the last repeat.

The steps of coordinating PSS2B and TCSC in a power system using the MOPSO algorithm are listed as follows:

First step: insert parameters of MOPSO algorithms (number of particles, repeat, $C2$, $C1$, and Rep)

Second step: insert the understudy power system parameters, such as generators, load, lines, and transformations

Third step: particles are given values randomly such that each particle consists of specific parameters of stabilizers and TCSC

Fourth step: after running the simulation and applying error, values of objective functions (ITAE and FD) are calculated

Fifth step: the values of best personal experience (P_{best}), best swarm experience, and dominant particles are determined

Sixth step: new particles are generated according to P_{best} and G_{best} values and dominant particles

Seventh step: the simulation is carried out again, and objective functions are calculated

Eighth step: in case ending conditions are not met, go to step five

Ninth step: end

Simultaneously minimizing both objective functions is the advantage of the MOPSO algorithm at high accuracy, and long simulation time duration is the disadvantage of this algorithm.

6. Simulation and Results Analysis

In this section, the obtained results from the simulation in MATLAB software are investigated. For this purpose, a 4-machine standard power system in Figure 12 has been selected as the sample system for studying and analyzing the interarea and local oscillations problem. In this system, two 900 MW generators are placed in each area, connected to each other via two 230 kV lines with 220 km in length. The information on lines, generators, and loads of this network is provided in the Appendix. In this system, the $G1$ generator

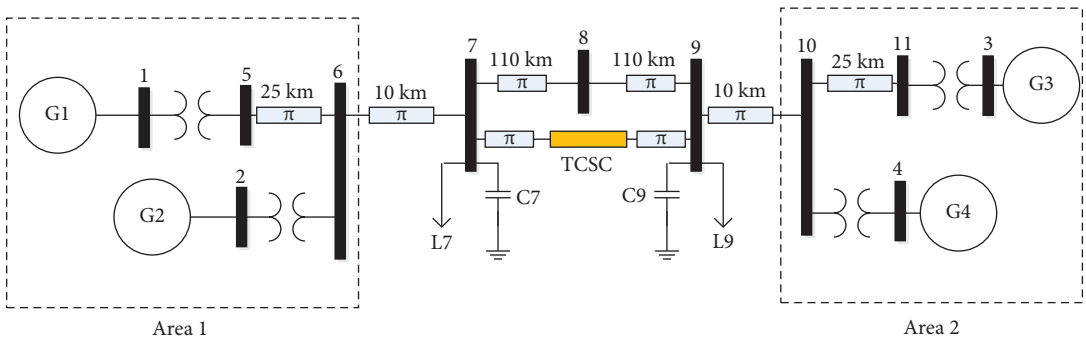

Figure 12: The understudy power system.

has been chosen as the reference generator, and the oscillations are calculated based on this generator's parameters.

The excitation system used in all generators is IEEE type AC4A. The block diagram of the AC4A excitation system is shown in Figure 13. The fast response of the AC4A excitation system helps to improve the stability of the power system.

The rating MVA and voltage are considered 900 MVA and 230 KV, respectively. In addition, the power system data are accumulated in Table 2.

In order to investigate the performance of the proposed control system, a three-phase symmetrical fault has been applied at the distance of 110 km from bus 7 with an endurance time of 200 ms. The three phase-to-ground faults are the most intense type of fault in a power system. If the power system could maintain itself in a stable condition, it could remain stable under another fault condition.

The problem of significant importance in a multiarea power system is that coordination should exist between installed stabilizers in each generator with other ones and the installed compensator in the connection line. In this case, in addition to interregional oscillations, the intraregional oscillations should also be damped quickly with the lowest amplitude. Since in the case of improper design of stabilizers, they are likely to negatively affect the performance of each other, increasing the intra and interregional oscillations and leading to the system's instability.

The studies are repeated under different loading conditions and in the form of two scenarios; the value of reactive power and produced reactive of each generator are indicated in Table 3.

In order to improve the system's stability, three methods are used.

(i) Making use of PSS2B stabilizers

(ii) Making use of TCSC compensators

(iii) Simultaneously making use of PSS2B stabilizer and TCSC compensator

It is worth mentioning that the PSS2B stabilizers are installed in *G*1 and *G*3 generators [35]. In order to optimally design the stabilizers and coordinate, the MOPSO algorithm is used. Also, nondominated sorting genetic algorithm (NSGAII) and multiobjective differential evolution (MODE) algorithms are used for solving the optimization problem. The parameters of the MOPSO algorithm and their variation amplitude are indicated in Table 4.

6.1. The Simulation Results. The parameters optimal adjustment is made to increase low-frequency oscillations damping together with settling time reduction with the maximum overshoot. After optimization by the MOPSO algorithm, the optimal values of PSS2B and TCSC parameters are estimated, indicated in Table 5.

In the transfer function of the PSS2B stabilizer's velocity transducer, the coefficients are selected to be $N = 1$, $T_9 = 0.1$, and $T_8 = 0.5$, and also $T_{w1} = T_{w2} = T_{w3} = 10$. The output signal limiter of this stabilizer is adjusted to be between −0.2 and 0.2 preunit. After the optimization by the MOPSO algorithm, the Pareto curve was obtained according to Figure 14, and it should be selected from the dominant particles of the final answer.

In Figure 14, the pareto fronts for the MOPSO, NSGAII, and MODE are shown by the blue circles, red square, and black cross markers respectively. As shown in this figure, the Pareto fronts for the proposed MOPSO has a lower value than other algorithms. Therefore, in the rest of the article, only the results of the MOPSO algorithm are displayed, and the results of the NSGAII and MODE algorithms were omitted.

In the presence of PSS2B, the values of ITAE and FD criteria are calculated to be 14.6 and 64.4, respectively. If the TCSC compensator is used, the values of these criteria will be 20.7 and 83.8, respectively. By coordinating PSS2B stabilizers and TCSC compensator, the ITAE value is 12.3, and the FD value is 44.6. The lower value of these two criteria indicates the stability of that power system's stability margin. The results indicate that a power system used with the simultaneous usage of PSS2B stabilizer, and TCSC had more performance than the two other stabilizing methods, able to maintain the FD and ITAE criteria at a lower level. In the following, the obtained results from the simulation are indicated in two scenarios.

6.2. The First Scenario. In the first scenario, the loading of the generator is indicated according to the first line of Table 2. By applying a 200 ms-symmetrical fault in the first second, the control system's performance in the realm of improving the power system's stability margin is evaluated. It is worth mentioning that the TCSC is placed in the middle of the connection line between two areas, and the fault occurred in another line. In the following, the interarea and local modes

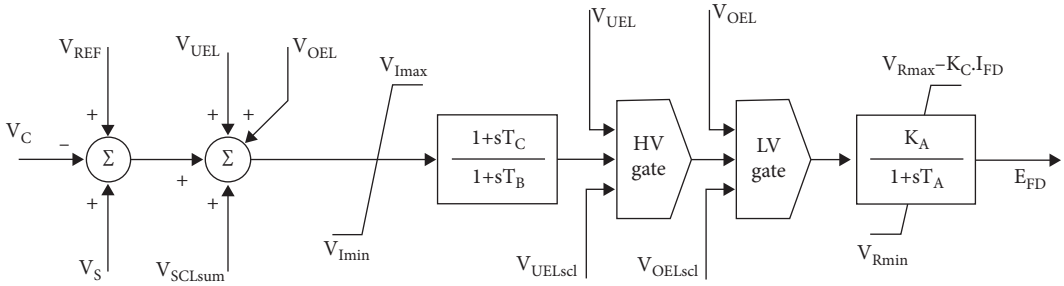

Figure 13: The IEEE type AC4A block diagram.

Table 2: The understudy power system specifications.

	*G*1	*G*2	*G*3	*G*4
R_a	0.00025	0.00025	0.00025	0.00025
x_d	1.8	1.8	1.8	1.8
x_q	1.7	1.7	1.7	1.7
$x_d^{'}$	0.3	0.3	0.3	0.3
$x_q^{'}$	0.55	0.55	0.55	0.55
$x_d^{''}$	0.25	0.25	0.25	0.25
$x_q^{''}$	0.25	0.25	0.25	0.25
$T_{do}^{'}$(s)	8	8	8	8
$T_{qo}^{'}$(s)	0.4	0.4	0.4	0.4
$T_{do}^{''}$(s)	0.03	0.03	0.03	0.03
$T_{qo}^{''}$(s)	0.05	0.05	0.05	0.05
K_A	200	200	200	200
T_A	0.02	0.02	0.02	0.02
H(s)	6.5	6.5	6.175	6.175

Table 3: The per-unit power of generators under different scenarios.

	P_1	Q_1	P_2	Q_2	P_3	Q_3	P_4	Q_4
First scenario	0.778	0.20	0.555	0.261	0.802	0.069	0.889	0.224
Second scenario	0.555	0.20	0.555	0.261	1.374	0.150	0.555	0.224

Table 4: The parameters of the MOPSO algorithm.

MODE	Population 100	Iteration 50	PCR 0.2	β_{min} 0.2	β_{max} 0.8	Rep 10
NSGAII	Population 100	Iteration 50	Pm 0.7	Pc 0.2	μ 0.02	Rep 10
MOPSO	Population 100	Iteration 50	C_1=C_2 2	V_{min} 0.9	V_{max} 0.4	Rep 10
		T_4 [0, 1]	T_3 [0, 1]	T_2 [0, 1]	T_1 [0, 1]	K [1, 30]

oscillation is indicated in Figure 15. The oscillations are based on rad/s.

According to Figure 15, the modes oscillations are defined in blue color dashed line in the case of PSS2B stabilizers employment; and if TCSC is used, they are defined in red color dashed line. Also, the results obtained from the simulation in the presence of PSS2B and TCSC

Table 5: The optimal values of PSS2B and TCSC stabilizer parameters.

	TCSC	*G*3	*G*1
K	21.73	23.68	26.71
T_1	0.83	0.31	0.56
T_2	0.74	0.19	0.43
T_3	0.43	0.51	0.84
T_4	0.92	0.66	0.51

simultaneously are demonstrated with black stretch lines. Figures 15(a) and 15(d) curves are the interarea and local modes oscillations, and Figures 15(b) and 15(c) curves are the intraregional modes variations. Since the *G*1 generator is considered the reference, all generators' rotational velocity variations are drawn based on that reference. As shown in Figure 15, in the presence of PSS2B stabilizer and TCSC, the interarea and local modes oscillations are damped quickly with the lowest variations. Also, power system oscillation will not be dampened if the stabilizer is not used (yellow dotted line) and the power system will become unstable. The maximum value of deviation amplitude from that of the oscillating modes for a power system merely using PSS2B stabilizer is 1.26×10^{-3} rad/s. However, in the case of using a TCSC compensator, the value of these oscillations is calculated to be 1.827×10^{-3} rad/s. Nevertheless, in the simultaneous presence of PSS2B and TCSC stabilizers, the value of this criterion has reduced to 1.168×10^{-3} rad/s. It is worth mentioning that the maximum variation amplitude is selected among the four curves in Figure 12 as the criteria of maximum deviation amplitude. The less this criteria value, the more stability margin the transmission line will have, capable of passing more electric energy. The stability method prefers a lower time for oscillations damping. The maximum time required for oscillations damping is 3.9 s for a power system with PSS2B and 5.7 s for a power system with TCSC; simultaneously, usage of PSS2B and TCSC and coordination between them is calculated to be 3.1 s.

6.3. The Second Scenario. A system has a proper level of performance in terms of stability that satisfies the required load power with an appropriate stability margin. In the second scenario, the performance of stabilizers is investigated under the condition of changing generators' output power. For this purpose, generators' active and reactive

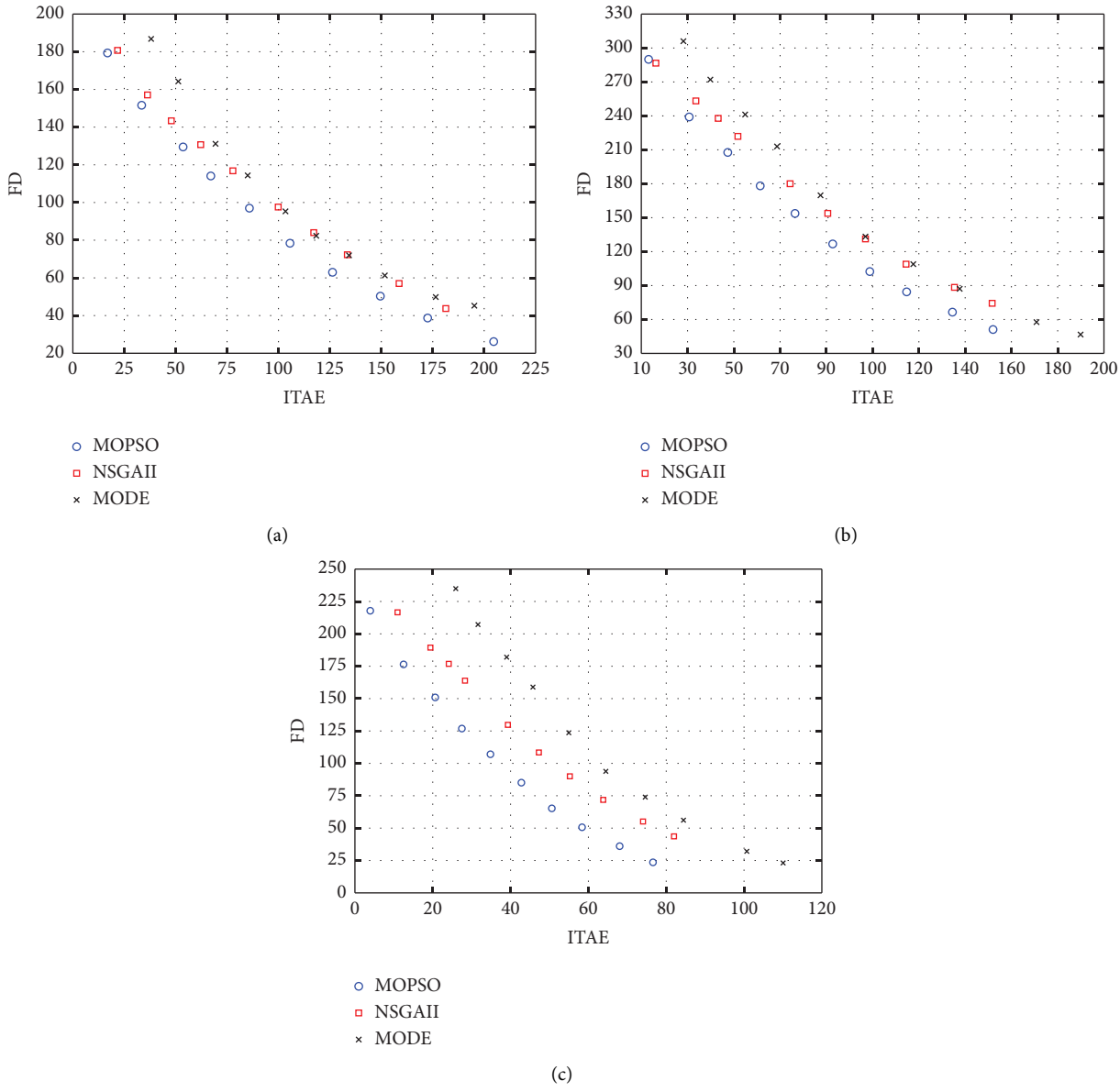

Figure 14: The dominant values at the presence of (a) PSS2B, (b) TCSC, (c) PSS2B, and TCSC, at the same time.

power is based on the second line of Table 2. The control systems' performance was evaluated by applying a three-phase symmetrical fault with an endurance time of 200 ms. The interarea and local modes oscillation in the second scenario are demonstrated in Figure 16.

The ITAE and FD criteria values are calculated to be 21.7 and 89.6 in the presence of PSS2B stabilizers. If a TCSC compensator is used, the values of these criteria are 31.9 and 115.3, respectively. By coordinating PSS2B stabilizers and TCSC compensator, the ITAE and FD values are 18.2 and 65.6, respectively. The lower value of the two criteria demonstrates its higher stability margin. Similar to the first scenario, in this scenario, a power system using PSS2B and TCSC simultaneously has a greater stability margin compared to the two other power systems. Also, its FD and ITAE criteria were lower in this case.

The maximum value of oscillation amplitude of the interregional and intraregional modes in the power system in which PSS2B stabilizers are solely employed is obtained at approximately 1.835×10^{-3} rad/sec. However, the maximum value of oscillation amplitude in the presence of compensator TCSC is obtained at 2.61×10^{-3} rad/sec. The maximum variation amplitude (oscillation amplitude) in the simultaneous presence of PSS2B stabilizer and TCSC is equal to 1.561×10^{-3} rad/s, which is lesser compared to the two previous power systems.

In the second scenario, the damping time of oscillatory modes was recalculated. The maximum damping time of oscillations in the power system with PSS2B stabilizers installed on $G1$ and $G3$ generators is approximately obtained 4.4 sec, and this value is equal to 4.6 s when employing TCSC in the communication line. However, in the simultaneous

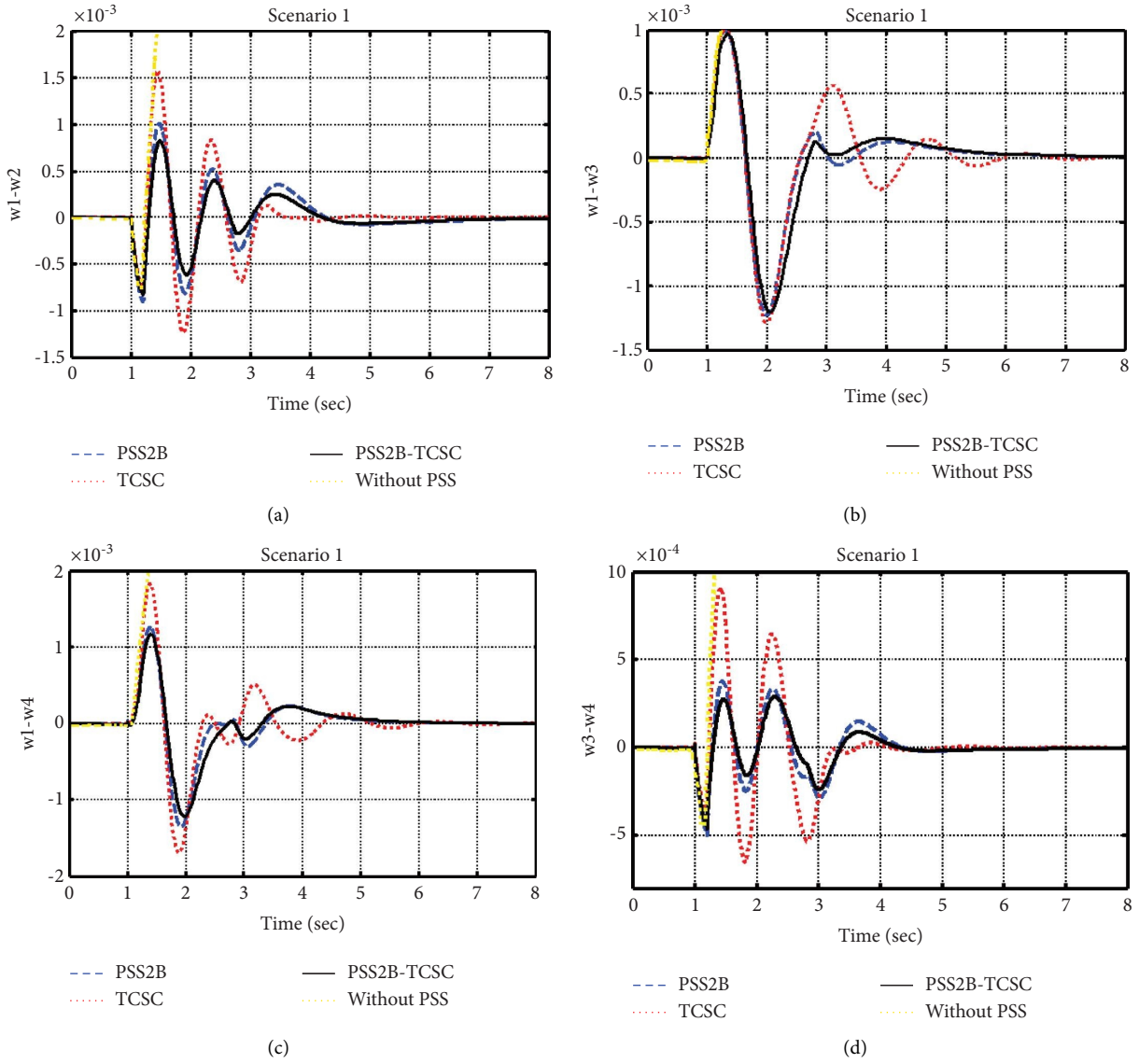

Figure 15: The interarea and local modes oscillations in the first scenario.

presence of PSS2B and TCSC and coordination between them by the MOPSO algorithm, the settling time of oscillations was obtained at 3.6 s, which is lesser compared to the two other control methods.

6.4. Simulation Results Analysis. In this section, the results obtained from the simulation are examined and analyzed in two scenarios. For this purpose, the FD, ITAE, oscillation damping time, and maximum deviation from reference value are compared for all stabilization methods. It must be noted that small values of these criteria indicate a greater stability margin of that power system. Besides, the simulation results of this paper were compared with the results of reference [37] which employed conventional PSS stabilizers and the TCSC compensator. In this article, the single-objective PSO algorithm was employed to coordinate PSSs and TCSC. In Figure 17, a bar chart of the ITAE criterion for different stability methods is indicated.

As indicated in Figure 14, in both scenarios, the minimum value ITAE belongs to the power system in which the PSS2B stabilizers and TCSC compensator are employed, which are optimized by the MOPSO algorithm. This indicates greater stability of the power system. Lesser values of ITAE indicate that the power system is capable of damping the oscillations in a lesser amount of time and with lesser amplitude. On the other hand, the maximum value of ITAE

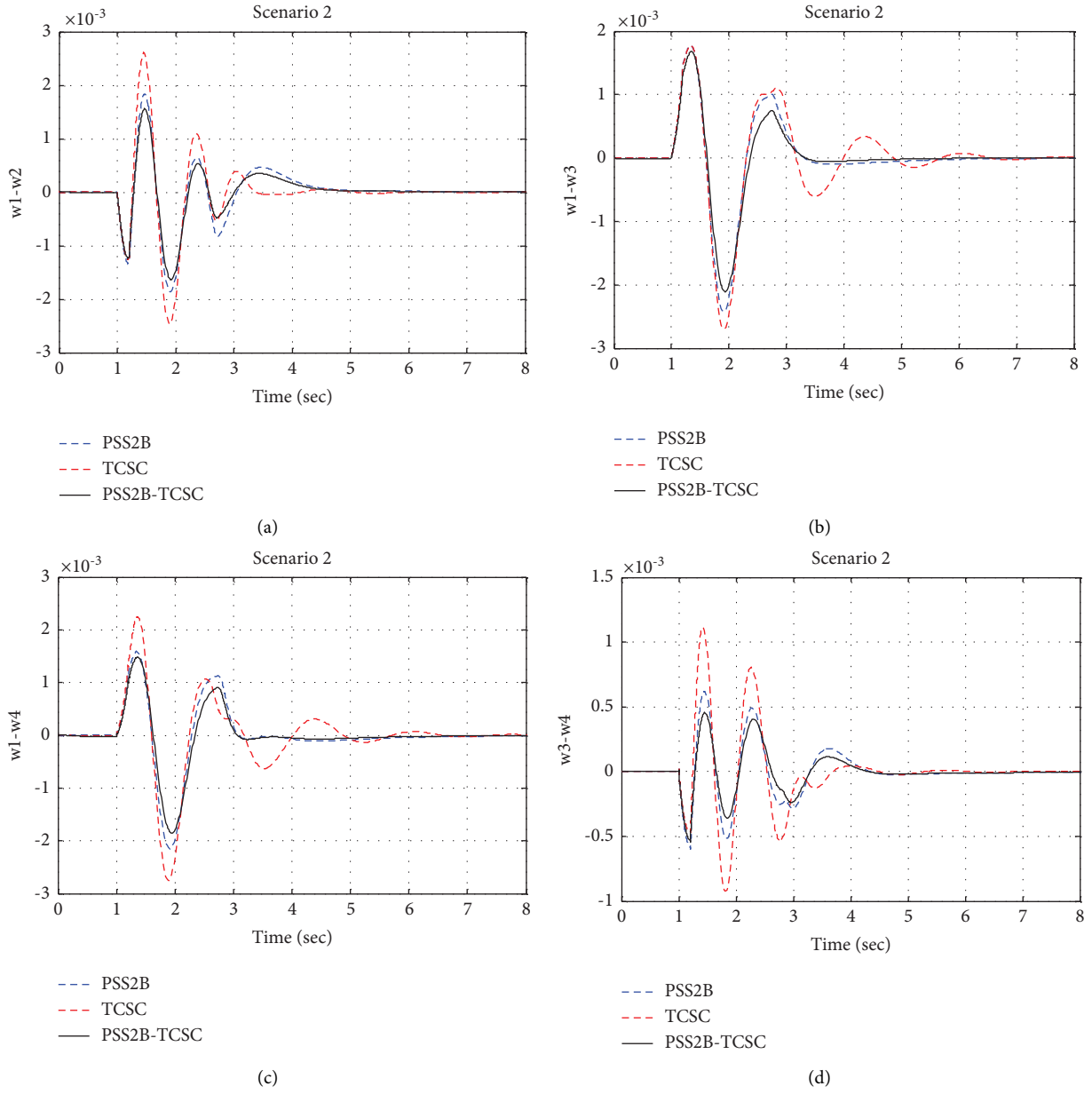

Figure 16: The interarea and local modes oscillations in the second scenario.

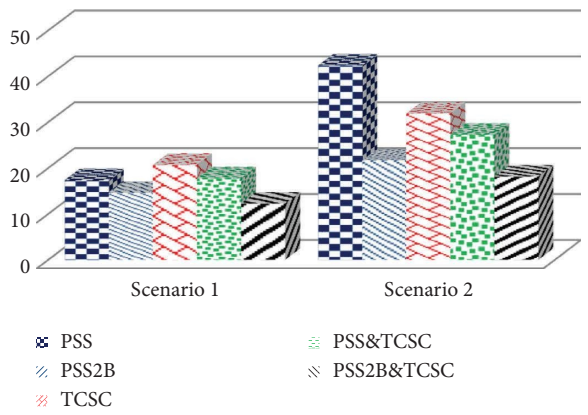

Figure 17: The values of the ITAE criterion.

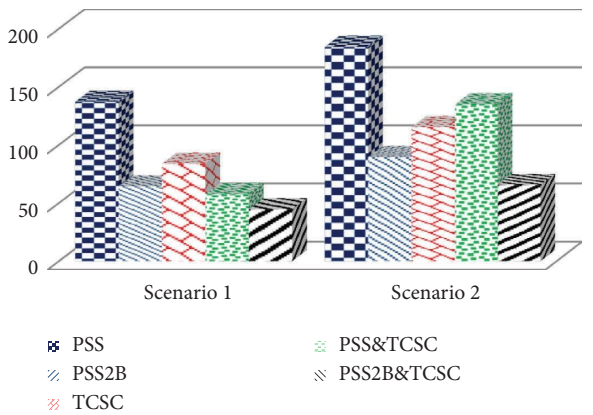

Figure 18: Values of the FD criterion.

Table 6: The ITAE and FD values.

		PSS	PSS2B	TCSC	PSS and TCSC	PSS2B and TCSC
ITAE	Scenario 1	17.4	14.6	20.7	17.8	12.3
	Scenario 2	42.4	21.7	31.9	27.3	18.2
FD	Scenario 1	137.1	64.4	83.8	57.6	44.6
	Scenario 2	184.4	89.6	115.3	134.9	65.6

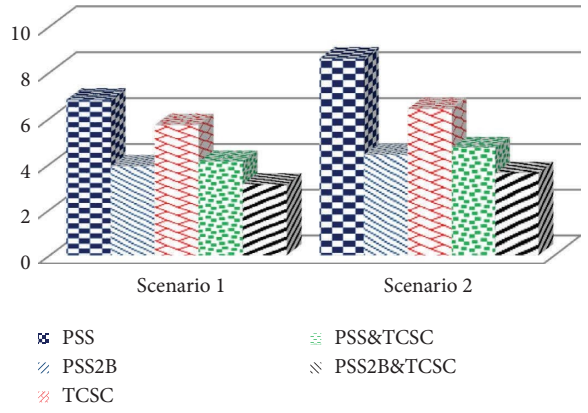

Figure 19: Damping time of oscillations.

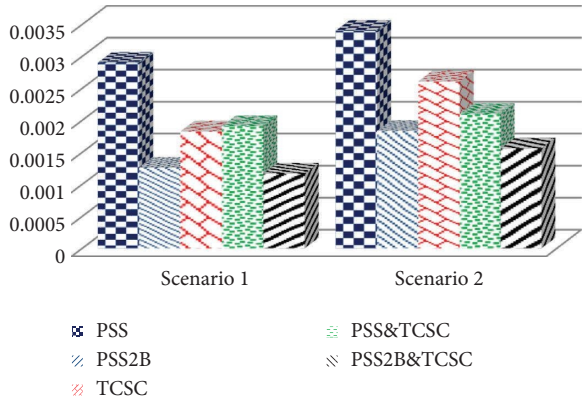

Figure 20: Maximum deviation from the reference value.

is in a power system in which the conventional stabilizer PSS is solely employed. The greater value of this criterion means lesser stability and a higher probability of instability. Figure 18 indicates the FD criterion of control systems in two scenarios.

The FD criterion that is mainly focused on the oscillations of each generator separately is obtained lesser than other control methods for PSS2B and TCSC optimized control systems in both scenarios. In the first scenario, the FD value of a power system with a combined compensator of PSS and TCSC is obtained lesser than that of a power system in which PSS2B is solely employed. However, in the second scenario, the opposite happened by changing the output power of the generators. In Table 6, the ITAE and FD values in two scenarios, and in the case of employing various control systems are indicated.

Another way to specify the superiority of a stabilizer over another is the settling time of oscillations. The faster a stabilizer could damp the oscillations caused by disturbances, the better its performance will be. In the following, the time required for oscillation damping in the understudy system is indicated in Figure 19.

The damping time of oscillations for the proposed control method of PSS2B and TCSC coordinated by the MOPSO algorithm at both scenarios *s* calculated less than 4 s, which is lesser time compared to that of other methods. The lesser the time required for damping oscillations, the lesser the instability probability in the next disturbances will be. As can be seen in Figure 19, the damping time of other control methods is more than 4 s, and the maximum value in both scenarios belongs to the power system in which only the PSS2B stabilizer is employed. Oscillation damping time

Table 7: The ITAE and FD values.

		PSS	PSS2B	TCSC	PSS & TCSC	PSS2B & TCSC
Settling time (sec)	Scenario 1	6.8	3.9	5.7	4.1	3.1
	Scenario 2	8.6	4.4	6.4	4.7	3.6
Maximum deviation (rad/sec)	Scenario 1	$2.90E-03$	$1.26E-03$	$1.83E-03$	$1.91E-03$	$1.17E-03$
	Scenario 2	$3.40E-03$	$1.84E-03$	$2.61E-03$	$2.10E-03$	$1.56E-03$

for this control system is obtained at approximately 6 s and more than 8 s for the first and second scenarios, respectively. Another criterion for comparing the performance of control methods is maximum oscillation amplitude [38–65]. The maximum deviation amplitude of oscillation is indicated in Figure 20.

The minimum value of this criterion belongs to the combined control system of PSS2B and TCSC, which are coordinated by the MOPSO algorithm. This matter can also approve the performance of the proposed control system. The maximum value of deviation amplitude for this control system is obtained at approximately 0.001 rad/sec and less than 0.002 rad/sec in the first and second scenarios, respectively. In Table 7, the maximum deviation and settling time for two scenarios are represented.

7. Conclusion

One of the essential subjects in power system problems is their dynamic stability, where losing stability leads to a power outage in various regions. This will consequently cause a lot of losses and damages to power equipments and consumers. Accordingly, special attention must be paid to stability. In this article, the stability of a four-machine power system located in two regions has been studied. To do this, the PSS2B stabilizers, along with TCSC, are employed in the power system. In order to improve the stability margin of the understudy power system, the PSS2B stabilizer and TCSC compensator are separately employed in the system in addition to the combined system of PSS2B and TCSC. In order to coordinate stabilizers and TCSC compensators, the MOPSO algorithm is employed, considering the ITAE and FD criterion as objective functions. Studies were carried out under two loading conditions in the form of two scenarios. Not getting trapped in local optimal points, high convergence speed, and high accuracy are the main features of the proposed algorithm which was used to solve the optimization problem. The correctness of the presented content was verified by performing optimization by two algorithms, MODE and NSGAII, and comparing it with the results of the proposed MOPSO algorithm. The optimization results showed that the MOPSO algorithm is more accurate than the other two algorithms. When the TCSC compensator was employed solely, these values were obtained 20.7 p.u. and 83.8 p.u. By coordinating the PSS2B stabilizer and TCSC compensator, the ITAE and FD values were calculated to be 12.3 p.u. and 44.6 p.u, respectively. In the second scenario, the values of ITAE and FD criteria in the presence of PSS2B stabilizers were obtained at 21.7 and 89.6, respectively, and obtained 31.9 and 115.3 in the case of using the compensator TCSC. By coordinating the PSS2B stabilizer and TCSC compensator, the ITAE and FD values were obtained at 18.2 and 65.6, respectively, which are lesser than those of the two control methods. The results indicate that compared to other stabilization methods, the power system in which the PSS2B stabilizer and TCSC are employed has a better performance and could keep the values of ITAE and FD criterion low. For future studies on the subject of the paper, it is proposed to coordinate the PSS2B stabilizer and the TCSC compensator in the power system in the presence of a wind farm with high penetration.

Data Availability

The data used to support the findings of this study are included within the paper.

Conflicts of Interest

The authors declare that they have no conflicts of interest.

Acknowledgments

This work was supported in part by an International Research Partnership "Electrical Engineering–Thai French Research Center (EE-TFRC)" under the project framework of the Lorraine Université d'Excellence (LUE) in cooperation between Université de Lorraine and King Mongkut's University of Technology North Bangkok and in part by the National Research Council of Thailand (NRCT) under Senior Research Scholar Program under grant no. N42A640328.

References

[1] M. Elsisi, "New design of robust PID controller based on meta-heuristic algorithms for wind energy conversion system," *Wind Energy*, vol. 23, no. 2, pp. 391–403, 2020.

[2] M. Elsisi and H. Abdelfattah, "New design of variable structure control based on lightning search algorithm for nuclear reactor power system considering load-following operation," *Nuclear Engineering and Technology*, vol. 52, no. 3, pp. 544–551, 2020.

[3] M. Eslami, H. Shareef, A. Mohamed, and M. Khajehzadeh, "An efficient particle swarm optimization technique with chaotic sequence for optimal tuning and placement of PSS in power systems," *International Journal of Electrical Power & Energy Systems*, vol. 43, no. 1, pp. 1467–1478, 2012.

[4] L. H. Hassan, M. Moghavvemi, H. A. F. Almurib, K. M. Muttaqi, and V. G. Ganapathy, "Optimization of power system stabilizers using participation factor and genetic algorithm," *International Journal of Electrical Power & Energy Systems*, vol. 55, pp. 668–679, 2014.

[5] S. Latif, S. Irshad, M. Ahmadi Kamarposhti, H. Shokouhandeh, I. Colak, and K. Eguchi, "Intelligent design of multi-machine power system stabilizers (PSSs) using improved particle swarm optimization," *Electronics*, vol. 11, no. 6, p. 946, 2022.

[6] S. Joshi and K. Pandya, "Optimal placement of TCSC for Total Transfer Capability enhancement using particle swarm optimization," in *Proceedings of the 8th International Conference on Advances in Power System Control, Operation and Management*, pp. 1–6, NY China, October 2009.

[7] A. Rezaee Jordehi, J. Jasni, N. Abd Wahab, M. Z. Kadir, and M. S. Javadi, "Enhanced leader PSO (ELPSO): a new algorithm for allocating distributed TCSC's in power systems," *International Journal of Electrical Power & Energy Systems*, vol. 64, pp. 771–784, 2015.

[8] M. Bakhshi, M. H. Holakooie, and A. Rabiee, "Fuzzy based damping controller for TCSC using local measurements to enhance transient stability of power systems," *International Journal of Electrical Power & Energy Systems*, vol. 85, pp. 12–21, 2017.

[9] D. Mondal, A. Chakrabarti, and A. Sengupta, "Optimal placement and parameter setting of SVC and TCSC using PSO to mitigate small signal stability problem," *International Journal of Electrical Power & Energy Systems*, vol. 42, no. 1, pp. 334–340, 2012.

[10] H. Shokouhandeh and M. Jazaeri, "Robust design of fuzzy-based power system stabiliser considering uncertainties of loading conditions and transmission line parameters," *IET Generation, Transmission & Distribution*, vol. 13, no. 19, pp. 4287–4300, 2019.

[11] X. Lei, E. Lerch, and D. Povh, "Optimization and coordination of damping controls for improving system dynamic performance," *IEEE Transactions on Power Systems*, vol. 16, pp. 473–480, 2010.

[12] H. Shokouhandeh and M. Jazaeri, "An enhanced and auto-tuned power system stabilizer based on optimized interval type-2 fuzzy PID scheme," *International Transactions on Electrical Energy Systems*, vol. 28, no. 1, p. e2469, 2018.

[13] H. Shokouhandeh, M. Jazaeri, and M. Sedighizadeh, "On-time stabilization of single-machine power system connected to infinite bus by using optimized fuzzy-PID controller," in *Proceedings of the 2014 22nd Iranian Conference on Electrical Engineering (ICEE)*, pp. 768–773, IEEE, Beijing China, May 2014.

[14] S. Panda, N. K. Yegireddy, and S. K. Mohapatra, "Hybrid BFOA–PSO approach for coordinated design of PSS and SSSC-based controller considering time delays," *International Journal of Electrical Power & Energy Systems*, vol. 49, pp. 221–233, 2013.

[15] H. Shayeghi, A. Safari, and H. A. Shayanfar, "PSS and TCSC damping controller coordinated design using PSO in multi-machine power system," *Energy Conversion and Management*, vol. 51, no. 12, pp. 2930–2937, 2010.

[16] E. Yasoubi, M. Sedighizadeh, and A. Siadatan, "Coordinated Design of PSS and TCSC Controllers using Colonal selection algorithm for stability enhancement of dynamical power system," in *Proceedings of the Industrial Technology (ICIT), IEEE International Conference on*, pp. 45–52, China, July 2017.

[17] H. Hasanvand, M. R. Arvan, B. Mozafari, and T. Amraee, "Coordinated design of PSS and TCSC to mitigate interarea oscillations," *International Journal of Electrical Power & Energy Systems*, vol. 78, pp. 194–206, 2016.

[18] S. M. Abd-Elazim and E. S. Ali, "Coordinated design of PSSs and SVC via bacterial foraging optimization algorithm in a multi-machine power system," *International Journal of Electrical Power & Energy Systems*, vol. 41, pp. 44–53, 2013.

[19] S. M. Abd-Elazim and E. S. Ali, "Power system stability enhancement via bacteria foraging optimization algorithm," *Arabian Journal for Science and Engineering*, vol. 38, no. 3, pp. 599–611, 2013.

[20] M. Tripathy and S. Mishra, "Coordinated tuning of PSS and TCSC to improve hopf bifurcation margin in multimachine power system by a modified bacteria foraging algorithmfied bacteria foraging algorithm," *International Journal of Electrical Power & Energy Systems*, vol. 66, pp. 97–109, 2015.

[21] D. K. Sambariya and R. Prasad, "Robust tuning of power system stabilizer for small signal stability enhancement using meta heuristic bat algorithm," *International Journal of Electrical Power & Energy Systems*, vol. 61, pp. 229–238, 2014.

[22] E. S. Ali, "Optimization of power system stabilizers using BAT search algorithm," *International Journal of Electrical Power & Energy Systems*, vol. 61, pp. 683–690, 2014.

[23] M. Pieroni, C. Marques, C. Campese et al., "Transforming a traditional product offer into PSS: a practical application," *Procedia CIRP*, vol. 47, pp. 412–417, 2016.

[24] M. A. Abdel-Moamen and N. P. Padhy, "Power flow control and transmission loss minimization model with TCSC for practical power networks," in *Proceedings of the 2003 IEEE Power Engineering Society General Meeting (IEEE Cat. No. 03CH37491)*, pp. 880–884, IEEE, New York China, June 2003.

[25] E. Gholipour and S. M. Nosratabadi, "A new coordination strategy of SSSC and PSS controllers in power system using SOA algorithm based on Pareto method," *International Journal of Electrical Power & Energy Systems*, vol. 67, pp. 462–471, 2015.

[26] R. Jalayer and B. T. Ooi, "Co-ordinated PSS tuning of large power systems by combining transfer function-eigen function analysis (TFEA), optimization, and eigenvalue sensitivity," *IEEE Transactions on Power Systems*, vol. 29, no. 6, pp. 2672–2680, 2014.

[27] R. K. Khadanga and J. K. Satapathy, "Time delay approach for PSS and SSSC based coordinated controller design using hybrid PSO–GSA algorithm," *International Journal of Electrical Power & Energy Systems*, vol. 71, pp. 262–273, 2015.

[28] B. P. Padhy, S. C. Srivastava, and N. K Verma, "A wide-area damping controller considering network input and output delays and packet drop," *IEEE Transactions on Power Systems*, vol. 32, no. 1, pp. 166–176, 2017.

[29] H. Shokouhandeh and M. Jazaeri, "An enhanced and auto-tuned power system stabilizer based on optimized interval type-2 fuzzy PID scheme," *Int Trans Electr Energ Syst*, vol. 28, no. 1, p. e2469, 2017.

[30] M. Elsisi, M. Soliman, M. A. S. Aboelela, and W. Mansour, "ABC based design of PID controller for two area load frequency control with nonlinearities," *TELKOMNIKA Indonesian Journal of Electrical Engineering*, vol. 16, no. 1, pp. 58–64, 2015.

[31] Z. Assi Obaid, L. Cipcigan, and M. T. Muhssin, "Power system oscillations and control: classifications and PSSs' design-methods: a review," *Renewable and Sustainable Energy Reviews*, vol. 79, pp. 839–849, 2017.

[32] E. V. Fortes, L. F. B. Martins, M. V. S. Costa, L. Carvalho, L. H. Macedo, and R. Romero, "Mayfly optimization algorithm applied to the design of PSS and SSSC-POD controllers for damping low-frequency oscillations in power systems," *International Transactions on Electrical Energy Systems*, vol. 2022, pp. 1–23, Article ID 5612334, 2022.

[33] Y. Nie, Y. Zhang, Y. Zhao, B. Fang, and L. Zhang, "Wide-area optimal damping control for power systems based on the ITAE criterion," *International Journal of Electrical Power & Energy Systems*, vol. 106, pp. 192–200, 2019.

[34] P. Rokni Nakhi and M. Ahmadi Kamarposhti, "Multi objective design of type II fuzzy based power system stabilizer for power system with wind farm turbine considering uncertainty," *International Transactions on Electrical Energy Systems*, vol. 30, no. 4, Article ID e12285, 2020.

[35] J. Kennedy and R. Eberhart, "Particle swarm optimization," in *Proceedings of the IEEE International Conference on Neural Networks*, pp. 1942–1948, Beijing China, April 1995.

[36] C. Coello and M. Salazar, "A proposal for multiple objective particle swarm optimization," *Congress on Evolutionary Computation*, vol. 20, pp. 1051–1056, 2002.

[37] V. Tayal and J. S. Lather, "Reduced order H ∞ TCSC controller & PSO optimized fuzzy PSS design in mitigating small signal oscillations in a wide range," *International Journal of Electrical Power & Energy Systems*, vol. 68, pp. 123–131, 2015.

[38] L. Qiu, L. He, H. Lu, and D. Liang, "Systematic potential analysis on renewable energy centralized co-development at high altitude: a case study in Qinghai-Tibet plateau," *Energy Conversion and Management*, vol. 267, Article ID 115879, 2022.

[39] L. Qiu, L. He, H. Lu, and D. Liang, "Pumped hydropower storage potential and its contribution to hybrid renewable energy co-development: a case study in the Qinghai-Tibet Plateau," *Journal of Energy Storage*, vol. 51, p. 104447, 2022.

[40] H. Chen, Y. Miao, Y. Chen, L. Fang, L. Zeng, and J. Shi, "Intelligent model-based integrity assessment of nonstationary mechanical system," *Journal of Web Engineering*, vol. 20, no. 2, 2021.

[41] L. Zhang, H. Zhang, and G. Cai, "The multi-class fault diagnosis of wind turbine bearing based on multi-source signal fusion and deep learning generative model," *IEEE Transactions on Instrumentation and Measurement*, vol. 71, pp. 1–12, 2022.

[42] L. Zhang, H. Zheng, G. Cai, Z. Zhang, X. Wang, and L. H. Koh, "Power-frequency oscillation suppression algorithm for AC microgrid with multiple virtual synchronous generators based on fuzzy inference system," *IET Renewable Power Generation*, vol. 16, no. 8, pp. 1589–1601, 2022.

[43] W. Zheng, X. Liu, and L. Yin, "Research on image classification method based on improved multi-scale relational network," *PeerJ Computer Science*, vol. 7, p. e613, 2021.

[44] Z. Ma, W. Zheng, X. Chen, and L. Yin, "Joint embedding VQA model based on dynamic word vector," *PeerJ Computer Science*, vol. 7, p. e353, 2021.

[45] J. Wang, J. Tian, X. Zhang et al., "Control of time delay force feedback teleoperation system with finite time convergence," *Frontiers in Neurorobotics*, vol. 16, p. 877069, 2022.

[46] H. Wang, K. Hou, J. Zhao, X. Yu, H. Jia, and Y. Mu, "Planning-Oriented resilience assessment and enhancement of integrated electricity-gas system considering multi-type natural disasters," *Applied Energy*, vol. 315, p. 118824, 2022.

[47] X. Xie and D. Chen, "Data-driven dynamic harmonic model for modern household appliances," *Applied Energy*, vol. 312, p. 118759, 2022.

[48] L. Guo, C. Ye, Y. Ding, and P. Wang, "Allocation of centrally switched fault current limiters enabled by 5G in transmission system," *IEEE Transactions on Power Delivery*, vol. 36, no. 5, pp. 3231–3241, 2021.

[49] C. Guo, C. Ye, Y. Ding, and P. Wang, "A multi-state model for transmission system resilience enhancement against short-circuit faults caused by extreme weather events," *IEEE Transactions on Power Delivery*, vol. 36, no. 4, pp. 2374–2385, 2021.

[50] T. Ni, D. Liu, Q. Xu, Z. Huang, H. Liang, and A. Yan, "Architecture of cobweb-based redundant TSV for clustered faults," *IEEE Transactions on Very Large Scale Integration Systems*, vol. 28, no. 7, pp. 1736–1739, 2020.

[51] Q. Zhang, C. Xin, F. Shen et al., "Human body IoT systems based on the triboelectrification effect: energy harvesting, sensing, interfacing and communication," *Energy & Environmental Science*, vol. 15, no. 9, pp. 3688–3721, 2022.

[52] Q. Zhang, Z. Liu, X. Jiang, Y. Peng, C. Zhu, and Z. Li, "Experimental investigation on performance improvement of cantilever piezoelectric energy harvesters via escapement mechanism from extremely Low-Frequency excitations," *Sustainable Energy Technologies and Assessments*, vol. 53, Article ID 102591, 2022.

[53] T. Sui, D. Marelli, X. Sun, and M. Fu, "Multi-sensor state estimation over lossy channels using coded measurements," *Automatica*, vol. 111, Article ID 108561, 2020.

[54] C. Lu, H. Zhou, L. Li et al., "Split-core magnetoelectric current sensor and wireless current measurement application," *Measurement*, vol. 188, Article ID 110527, 2022.

[55] J. Kang, Y. Xue, J. Yang et al., "Realizing two-electron transfer in $Ni(OH)_2$ nanosheets for energy storage," *Journal of the American Chemical Society*, vol. 144, no. 20, pp. 8969–8976, 2022.

[56] X. Xu, D. Niu, L. Peng, S. Zheng, and J. Qiu, "Hierarchical multi-objective optimal planning model of active distribution network considering distributed generation and demand-side response," *Sustainable Energy Technologies and Assessments*, vol. 53, Article ID 102438, 2022.

[57] Y. Xu, X. Chen, H. Zhang et al., "Online identification of battery model parameters and joint state of charge and state of health estimation using dual particle filter algorithms," *International Journal of Energy Research*, vol. 46, no. 14, pp. 19615–19652, 2022.

[58] C. Lu, Q. Liu, B. Zhang, and L. Yin, "A Pareto-based hybrid iterated greedy algorithm for energy-efficient scheduling of distributed hybrid flowshop," *Expert Systems with Applications*, vol. 204, p. 117555, 2022.

[59] H. Chen and S. Li, "Multi-sensor fusion by CWT-PARAFAC-IPSO-SVM for intelligent mechanical fault diagnosis," *Sensors*, vol. 22, no. 10, p. 3647, 2022.

[60] B. Li, C. Li, Y. Zhang, Y. Wang, D. Jia, and M. Yang, "Grinding temperature and energy ratio coefficient in MQL grinding of high-temperature nickel-base alloy by using different vegetable oils as base oil," *Chinese Journal of Aeronautics*, vol. 29, no. 4, pp. 1084–1095, 2016.

[61] X. Cui, C. Li, Y. Zhang et al., "Grindability of titanium alloy using cryogenic nanolubricant minimum quantity lubrication," *Journal of Manufacturing Processes*, vol. 80, pp. 273–286, 2022.

[62] A. E. Anqi, C. Li, H. A. Dhahad et al., "Effect of combined air cooling and nano enhanced phase change materials on thermal management of lithium-ion batteries," *Journal of Energy Storage*, vol. 52, Article ID 104906, 2022.

[63] Z. Duan, L. I. Changhe, Y. Zhang et al., "Mechanical behavior and Semiempirical force model of aerospace aluminum alloy milling using nano biological lubricant," *Frontiers of Mechanical Engineering*, vol. 1, 2022.

[64] Z. J. Duan, C. H. Li, Y. B. Zhang et al., "Milling surface roughness for 7050 aluminum alloy cavity influenced by nozzle position of nanofluid minimum quantity lubrication," *Chinese Journal of Aeronautics*, vol. 34, no. 6, pp. 33–53, 2021.

[65] M. Yang, C. Li, Y. Zhang et al., "Research on microscale skull grinding temperature field under different cooling conditions," *Applied Thermal Engineering*, vol. 126, pp. 525–537, 2017.